Pergamon

0042-6989(95)00120-4

Vision Res. Vol. 36, No. 3, pp. 425–430, 1996

0042-6989/96 $15.00 + 0.00

Short Communication

A Second-order Pattern Reveals Separate Strategies for Encoding Orientation in Two-dimensional Space and Space–Time

P. W. McOWAN,* A. JOHNSTON*

Received 29 November 1994; in revised form 10 April 1995

We measured the perceived spatial orientation of the low contrast regions of contrast modulated sine gratings. Subjects make systematic errors which depend upon the carrier spatial frequency and the angle between the carrier grating and the modulation. The results for the spatial orientation task are compared with a motion domain analogue. The difference in the pattern of results for these two tasks suggests there exist separate strategies for encoding orientation in two-dimensional space and space–time.

Orientation Second-order Contrast modulation Rectification

INTRODUCTION

Neurophysiological investigations of the visual cortex reveals populations of cells which respond well only when the retinal image contains spatial structure at a particular orientation (Hubel & Wiesel, 1977). This concept of orientation as a fundamental measure in visual perception has been generalized and extended to encompass visual domains beyond that of orientation in two-dimensional space through the formalism of the plenoptic function (De Yoe & Van Essen, 1988; Adelson & Bergen, 1991). This representation describes the input from the environment to the visual system as a multi-dimensional function of direction, time, wavelength and viewpoint and so allows the construction of the basic measures of the visual process as the measurement of orientation in this multi-dimensional space. Computational models of motion perception (van Santen & Sperling, 1985; Watson & Ahumada, 1985; Heeger, 1987; Adelson & Bergen, 1985; Wilson, Ferrera & Yo, 1992; Johnston, McOwan & Buxton, 1992) and stereo disparity (Ohzawa, De Angelis & Freeman, 1990), use measures of an appropriately defined orientation to extract their required signals.

It has become commonplace to use the space–time plot as a device to represent stimulus motion (Fig. 1) where the velocity becomes an orientation in a domain spanned by space and time. There is thus a strong analogy between motion as orientation in space–time and spatial orientation in the two-dimensional (2D) space domain. The physiological evidence suggests spatial orientation is encoded as a distribution of activity in an array of linear, orientation tuned cells. Consequently, many models of motion perception propose a population of linear, spatiotemporally tuned filters which have receptive fields that are oriented in space–time. The output from each of these filters is then squared to derive a phase independent measure of the energy at their selected spatiotemporal frequency. These motion energy output components are then combined over the filter population, for example using a least squares fit (Heeger, 1987), to produce the required velocity.

Energy models rely on measurements of the orientation of the Fourier power spectrum of the stimulus (van Santen & Sperling, 1985; Watson & Ahumada, 1985; Heeger, 1987; Adelson & Bergen, 1985; Wilson *et al.*, 1992; Ohzawa *et al.*, 1990; Landy & Bergen, 1991), and are underpinned by an assumption that the Fourier transform of the stimulus consists of energy components positioned on a plane through the origin of frequency space. This requirement does not however hold in the case of second-order stimuli (Chubb & Sperling, 1988). In this class of stimuli the Fourier energy components that constitute the stimuli do not all lie on planes through the frequency space origin, thus the standard energy model cannot operate reliably.

In an effort to modify the energy model to deal with this important class of second-order stimuli a point-wise non-linearity, such as full-wave rectification, is introduced prior to the energy stage (Chubb & Sperling,

*Department of Psychology, University College London, Gower Street, London WC1E 6BT, England.

1988). This non-linear stage has the effect of demodulating the spectrum of the stimulus, returning the energy components to the orientation through the frequency space origin as required for the energy model. This non-linear pre-processing stage has been suggested as a mechanism to account for the perception of second-order stimuli in both space–time (Chubb & Sperling, 1988) and 2D space (Chubb, Econopouly & Landy, 1994; Sutter, Sperling & Chubb, 1995). One second-order stimulus that has been studied in the motion domain (Johnston & Clifford, 1995a; Derrington & Henning, 1993) is the contrast modulated sine grating $I(x,t)$, equation (1).

$$I(x,t) = (1 + M \sin(k_{mx}x + k_{mt}t))\sin(k_{cx}x + k_{ct}t) \quad (1)$$

where k_{mx} and k_{mt} are the spatial and temporal frequencies and M the modulation depth, ranging from 0 to 1, of the modulating grating, and k_{cx} and k_{ct} the spatial and temporal frequencies of the carrier grating. Figure 2 shows a number of possible forms of this second-order stimulus and the resulting structure of their Fourier energy spectra. The carrier grating moves the Fourier energy components associated with the modulation envelope away from the frequency space origin as shown diagrammatically in Fig. 2(a–f). Higher carrier spatial frequencies give rise to a greater displacement of the modulation energy from the origin. The orientation of the carrier grating determines the precise location of the energy components within the Fourier plane.

Applying a realisation of a single spatiotemporally tuned component of the Fourier energy model (Adelson & Bergen, 1985) to this contrast modulated sine grating stimulus produces the results shown in Fig. 3. As can be seen the model does not signal the space–time orientation of the modulation envelope in this stimulus. The energy model instead picks up and signals the orientation of the carrier grating which, in this case, is vertical. However augmenting the motion energy model with a non-linear pre-filter would predict that the motion of the modulating grating would be perceived veridically as rectification demodulates the energy of the modulation envelope back about the origin. When this motion stimulus is measured psychophysically however, there is a structured motion field and systematic underestimation of the speed of the low contrast regions of the modulations (Johnston & Clifford, 1995a).

An alternative approach to the Fourier energy method of modelling motion perception is to calculate a well-conditioned measure of the spatiotemporal gradients in the stimulus (Johnston *et al.*, 1992; Johnston & Clifford, 1995a, b). The predictions of the gradient motion model for contrast modulated gratings are shown in Fig. 4. The matching speed predicts the perceived speed of the low contrast regions of the modulation envelope. In the graph shown in Fig. 4 the dotted line at 1 deg/sec denotes veridical perception and the dotted line at 0 deg/sec the perception of a static envelope. The variation of carrier velocity produces a corresponding change in the angle of the carrier grating represented in a space–time plot. In the stimulation the modulation envelope is held constant at 1 deg/sec, that is at a +45 deg orientation in the space–time plot. A carrier velocity of 1 deg/sec places the modulating and carrier gratings at the same +45 deg orientation. A carrier velocity of −1 deg/sec places the

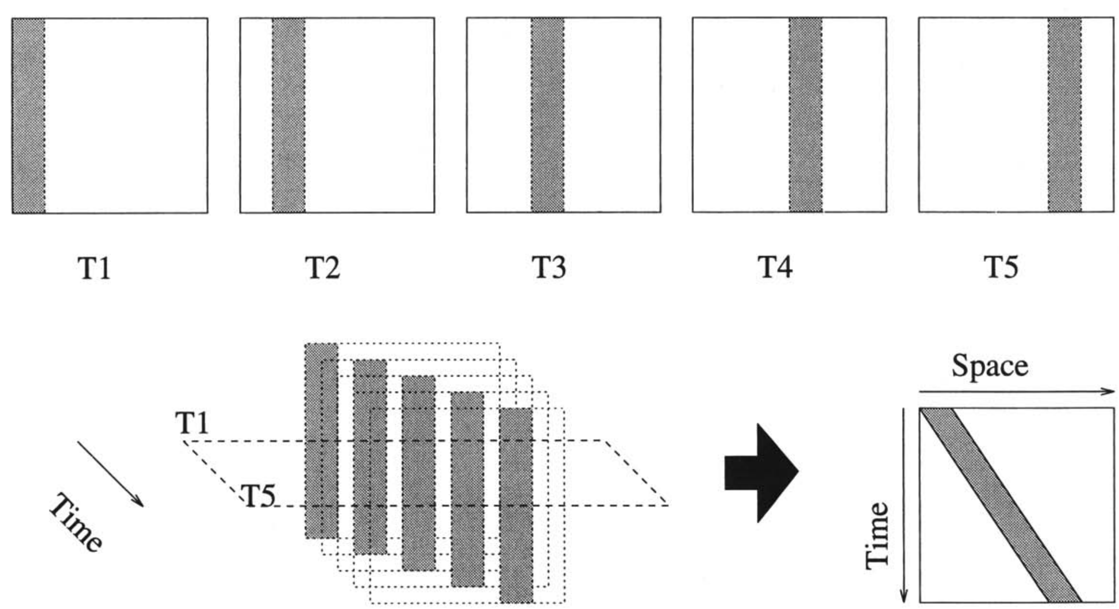

FIGURE 1. Motion as orientation in space–time. The vertical bar moves continuously to the right and is shown at the top in five "snapshots" at times T1–T5. All of the instants comprising this motion are then stacked in the correct chronological order to form a space–time solid. Because the spatial stimulus is vertically uniform, and therefore spatially one-dimensional, taking any horizontal slice through this space–time solid, as shown, produces the representative space–time graph on the right. The velocity of the stimulus is encoded as the orientation of structure in this domain spanned by space and time. Zero velocity is represented by vertical structure parallel to the time axis and reduced velocity corresponds to an orientation moving closer to vertical.

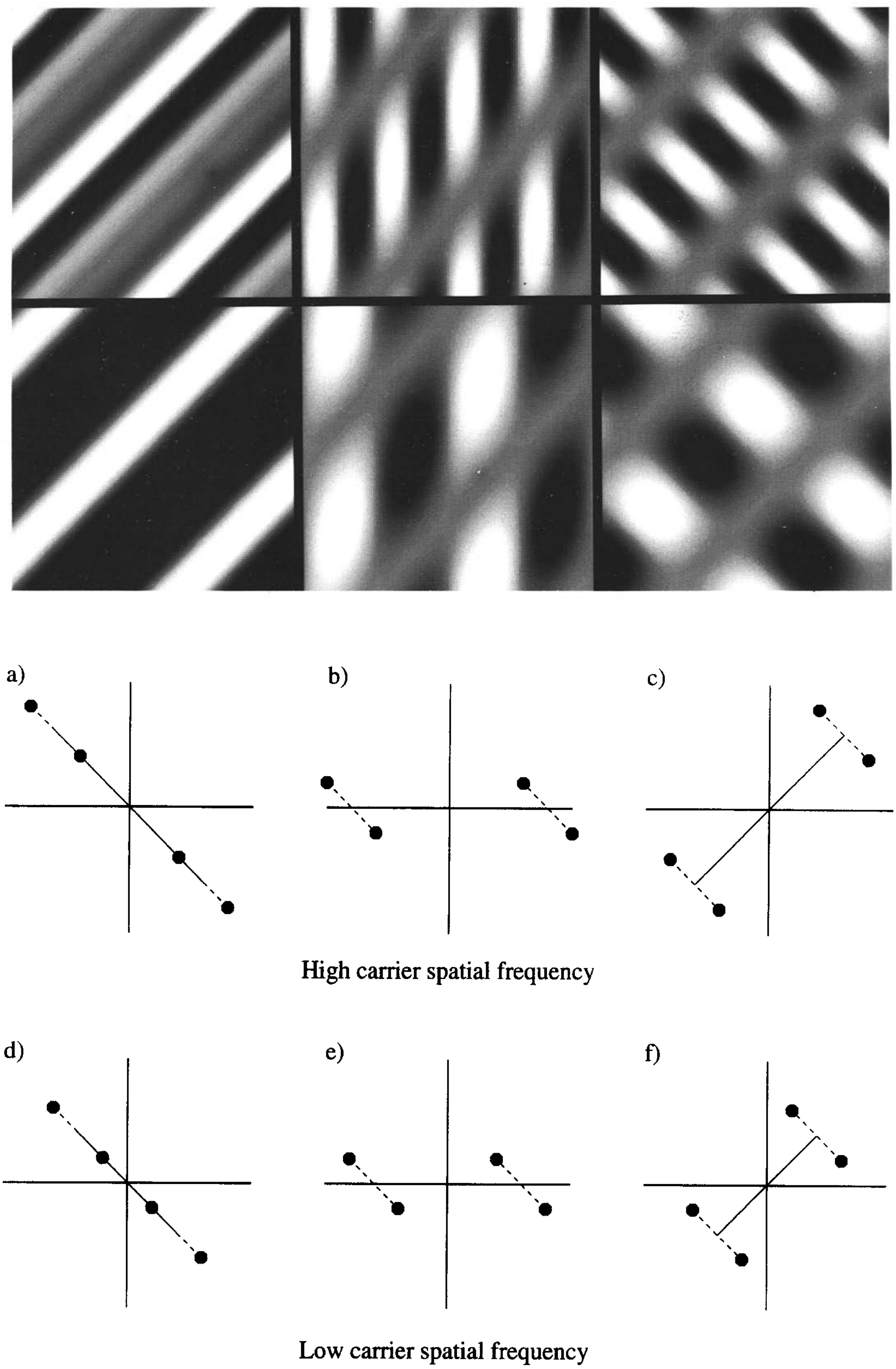

FIGURE 2. The contrast modulated sine gratings used as stimuli in this investigation and a schematic diagram of their Fourier energy spectra. The contrast modulated grating is depicted along with a corresponding schematic showing the distribution of energy about the frequency space origin of the Fourier spectra (a–f). The top set of stimuli have a high carrier spatial frequency (a, b and c), the stimuli shown beneath have a low carrier spatial frequency (c, d and e). In all the stimuli shown the modulation envelope orientation is held constant at +45 deg, angles being measured positive clockwise from vertical. The three carrier orientation conditions shown are with the carrier grating at 45 deg, parallel to the modulation orientation (a and d), the carrier grating vertical at 0 deg (b, e), and the carrier grating orientation at −45 deg, orthogonal to the modulation (c, f). It may be observed that for the vertical carrier (stimuli b and e), the perceived orientation of the low contrast areas of the modulation envelope seem to be oriented more towards the vertical than for the other carrier orientations shown. This effect is more pronounced at low carrier spatial frequency (e).

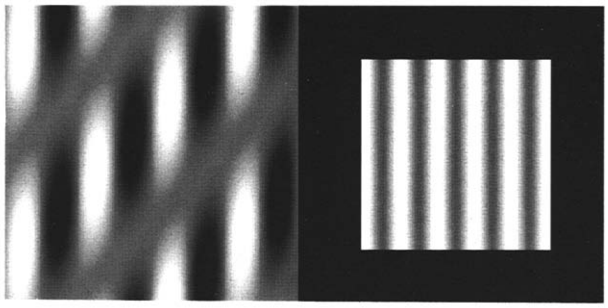

FIGURE 3. The results of applying a spatiotemporally tuned component of the standard Fourier energy model (as specified in Adelson & Bergen, 1985) to the contrast modulated sine grating. This motion stimulus is shown in the space–time plot in the left panel. In this diagram space is represented horizontally and time increases vertically down the page. Thus the stimulus as shown corresponds to the low contrast regions moving to the left and a static carrier. The output from a standard Fourier energy model when applied to this space–time stimulus is shown in the right panel. The Fourier energy model output, without the use of an explicit rectification, is unable to extract the orientation of the contrast modulation envelope.

carrier and modulation orientations orthogonal to each other. The carrier velocity at 0 deg/sec is static, which corresponds to a vertical grating in the space–time plot.

Where present, the predicted misperception of velocity increases as a function of the carrier spatial frequency. As the carrier velocity, represented as orientation in space–time, moves through 90 deg from the +45 to −45 orientation conditions there is a monotonic increase in the misperception of speed. Each of these predictions is confirmed by the psychophysical data (Johnston & Clifford, 1995a) and therefore Fig. 4 indicates the pattern of results expected for the motion task. To test if the analogy of measuring orientation in 2D space and space–time holds we can measure the perceived spatial orientation of the low contrast regions of the second-order pattern in the 2D space domain and compare the results in this task with the results for the motion task.

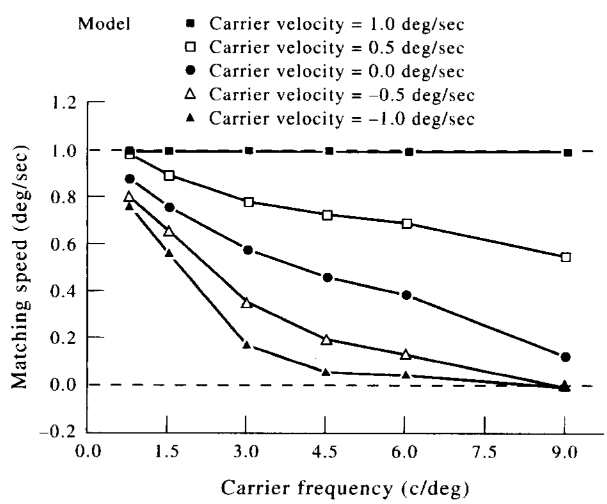

FIGURE 4. Predictions from a spatiotemporal multi-channel gradient model of motion perception for a contrast modulated sine grating.

METHODS AND RESULTS

Equipment

Stimuli were generated by a Sun Sparcstation LX and were presented on a display with a mean luminance of 39.0 cd/m^2. Prior to the undertaking the experiments the screen was carefully gamma corrected using a spot photometer UDT OPTOMETER S370.

The perceived orientation of the low contrast regions of the contrast modulated gratings was measured using an adaptive method of constants (Watt & Andrews, 1981). Subjects, PM and a naive subject SP, were asked to compare the orientation of the low contrast regions of the contrast modulated sine grating with the orientation of a sine wave grating held throughout the experiments at a fixed orientation of +45 deg. The orientation of the modulation envelope was varied about the +45 deg direction from trial to trial using the adaptive procedure. The point of subjective equality (PSE) on the psychometric function is taken as a measure of the difference in orientation of the modulation envelope, from the true value of +45 deg, that is required to null any illusory change present in the perceived orientation. This experimental procedure in effect implements a nulling paradigm using the method of constant stimuli, rather than the method of adjustment which is the more commonly used nulling technique.

The stimuli were presented for 2 sec in two circular windows of 4.74 deg diameter, centres separated by 6.5 deg, with a prominent fixation point half way between the two apertures. The stimuli were viewed binocularly with the side of presentation and grating spatial phase varied randomly over trials. All stimuli were presented on a uniform background at the mean luminance of the sine grating with the sine grating constrast set equal to the modulation depth of the envelope, $M = 0.8$. Perceived modulation orientation was measured over a two octave range of carrier spatial frequencies, 0.63, 0.84, 1.26, 1.47, 1.89, 3.78 and 7.56 c/deg, and five different orientations of carrier grating. All angles were measured as positive clockwise from the vertical and the standard errors are shown at each data point on the graph. The spatial frequency of the contrast modulation envelope and the fixed +45 deg sine grating were set constant at a value of 0.84 c/deg.

The PSEs measured as a function of both the spatial frequency and orientation of the carrier grating are shown in Fig. 5(a and b) for the two observers. The +45 deg carrier orientation condition places modulating and carrier gratings parallel, and the −45 deg condition places modulation and carrier gratings orthogonal to each other. The 0 deg carrier orientation condition corresponds to a spatially vertical carrier. Where present the misperception of the orientation of the low contrast regions of the envelope decreases toward veridical as carrier spatial frequency increases. As the carrier orientation moves through 90 deg from the +45 to −45 deg conditions the misperception increases from being approximately veridical, to peak for the vertical carrier

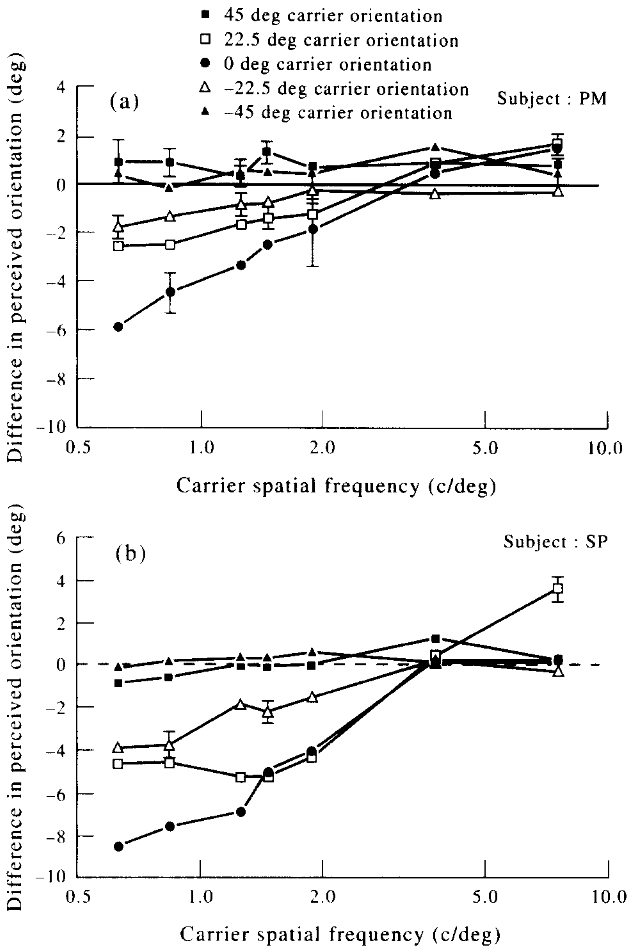

FIGURE 5. Results for two subjects, PM (a) and naive subject SP (b), for the spatial orientation task. To allow comparison between domains the symbols on the graphs correspond to the same angles between carrier and modulation as in the space–time realisation shown in Fig. 4. The ordinate describes the difference in the perceived orientation of the envelope expressed relative to the orientation of the fixed reference sine grating at +45 deg. A minus value refers to an anticlockwise shift in the perceived modulation orientation.

orientation, and then reduces to return again to veridical. For one subject, PM, there is a tendancy for the +45 and −45 deg conditions to be oriented toward the horizontal relative to the fixed grating for all carrier spatial frequencies. For subject SP there is evidence for a bias towards the horizontal in the +22.5 deg condition at the highest carrier spatial frequency. To allow comparison the symbols on these graphs, Fig. 5(a and b), correspond to the same angles between carrier and modulation orientations as in the modelled results of the space–time realisation of the similar velocity matching task illustrated in Fig. 4.

DISCUSSION

An energy model with a rectifying pre-filter step implementing a carrier demodulation could, in principle, correctly compute the 2D spatial orientation, but it would not predict the data at all carrier spatial frequencies measured. The most dramatic misperceptions of orientation occur with low carrier spatial frequencies. The modulation envelope spatial frequency was set throughout at 0.84 c/deg. For carrier spatial frequencies less than this value the stimulus, though technically still second-order, with the envelope orientation displaced from the frequency origin albeit only slightly, may be considered to be tending toward being first-order. In this case the low frequency carrier may be regarded as providing a luminance bed that is locally constant relative to the envelope modulations. An energy model, even without the pre-filter non-linearity required to demodulate the higher carrier frequency stimuli, could be seen as a strong candidate for a mechanism which could extract the orientation. However the visual system would, in this case, be expected to correctly signal the modulation orientation. Thus the energy model would not be able to account for the measured biases in perceived orientation.

The main difference in approach taken here is that the stimulus pattern is viewed as a surface, where the height of the surface is determined by the image brightness. Usually contrast modulated patterns are viewed in terms of the way they may be constructed from sine gratings which is given by their Fourier transforms. Whether they are considered to be constructed by adding component gratings moving in opposite directions or by multiplication of one signal by another depends upon whether the spectral components are grouped via a mirror symmetry through the origin or as a pair of local orientations. There is no *a priori* grouping in the transform itself. Indeed whether we see this complex waveform as being composed of Fourier components is a matter of choice and convenience. The visual system need not extract these constituent parts of the signal and for the task employed here, which involves judgments of local orientation, it is not clear how decomposition of the brightness surface into components with various globally defined orientations would be helpful.

A gradient model which fits the motion domain data well (Johnston & Clifford, 1995a) also generates incorrect predictions for 2D space, though it does predict the presence of rotations in perceived orientation towards the vertical. If the same mechanisms were employed to compute orientation in space–time and 2D space the

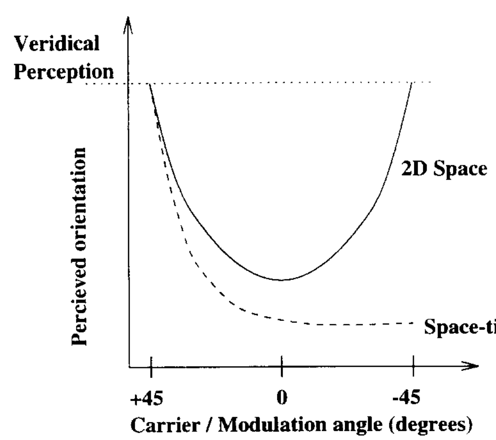

FIGURE 6. Illustration of the two distinct forms of dependency of perceived orientation of the low contrast regions of the modulation envelope as a function of carrier orientation for 2D space and space time.

pattern of results in Fig. 5(a and b) should be similar to that shown in Fig. 4. However, in the motion task, errors in perceived speed increase with carrier speed and spatial frequency while, in the spatial task, errors in perceived orientation peak for a vertical carrier and decrease with increasing spatial frequency. These two distinct domain specific trends of perceived orientation as a function of carrier orientation are summarized in Fig. 6.

Although a simple transfer of methods for measuring orientation between the motion and 2D space domains would be convenient this strategy is not supported by the psychophysical evidence presented here. In particular, approaches to modelling motion perception which draw heavily on the generalization of putative schemes for encoding orientation in 2D spatial patterns, e.g. proposing a population of linear filters which cover a range of orientations in space–time, need to be re-evaluated in the light of clear differences in visual processing in the two domains. This functional dissociation may reflect differences in the distribution of filters that are available in the two domains, many more orientation tuned filters are available in 2D space, and physical constraints such as the requirement of causality in the temporal domain.

REFERENCES

Adelson, E. H. & Bergen, J. R. (1985). Spatiotemporal energy models for the perception of motion. *Journal of the Optical Society of America A*, *2*, 284–299.

Adelson, E. H. & Bergen, J. R. (1991). The plenoptic function and the elements of early vision. In Landy, M. S. & Movshon, J. A. (Eds), *Computational models of visual processing* (pp. 2–20). Cambridge MA: MIT Press.

Chubb, C. & Sperling, G. (1988). Drift balanced random dot stimuli; a general basis for studying non Fourier motion. *Journal of the Optical Society of America A*, *5*, 1986–2007.

Chubb, C., Econopouly, J. & Landy, M. S. (1994). Histogram contrast analysis and visual segregation of IID textures. *Journal of the Optical Society of America A*, *11*, 2350–2374.

Derrington, A. M. & Henning, B. G. (1993). Linear and non-linear mechanisms in pattern vision. *Current Biology*, *3*, 800–803.

De Yoe, E. A. & Van Essen, D. C. (1988). Concurrent processing streams in monkey visual cortex. *Trends in Neuroscience*, *11*, 219–226.

Heeger, D. J. (1987). Model for the extraction of image flow. *Journal of the Optical Society of America A*, *4*, 1455–1471.

Hubel, D. H. & Wiesel, T. N. (1977). Functional architecture of the macaque monkey visual cortex. *Proceedings of the Royal Society of London B*, *198*, 1–59.

Johnston, A. & Clifford, C. W. G. (1995a). Perceived motion of contrast modulated gratings: predictions of the Multi-channel Gradient model and the role of full wave rectification. *Vision Research*, *35*, 1771–1783.

Johnston, A. & Clifford, C. W. G. (1995b). A unified account of three apparent motion illusions. *Vision Research*, *35*, 1109–1123.

Johnston, A., McOwan, P. W. & Buxton, H. (1992). A computational model of the analysis of some first-order and second-order motion patterns by simple and complex cells. *Proceedings of the Royal Society of London B*, *250*, 297–306.

Landy, M. S. & Bergen, J. R. (1991). Texture segregation and orientation gradient. *Vision Research*, *31*, 679–691.

Ohzawa, I., De Angelis, G. C. & Freeman, R. D. (1990). Stereoscopic depth discrimination in the visual system; neurons ideally suited as disparity detectors. *Science*, *249*, 1037–1040.

van Santen, J. P. H. & Sperling, G. (1985). Elaborated Reichardt detectors. *Journal of the Optical Society of America A*, *2*, 300–321.

Sutter, A., Sperling, G. & Chubb, C. (1995). Measuring the spatial frequency selectivity of second-order texture mechanisms. *Vision Research*, *35*, 915–924.

Watson, A. B. & Ahumada, A. J. (1985). Model of human visual-motion sensing. *Journal of the Optical Society of America A*, *2*, 322–341.

Watt, R. J. & Andrews, D. P. (1981). APE: Adaptive Probit Estimation of psychometric functions. *Current Psychological Reviews*, *1*, 205–214.

Wilson, H. R., Ferrera, V. P. & Yo, C. (1992). A psychophysically motivated model for two-dimensional motion perception. *Visual Neuroscience*, *9*, 79–97.

Acknowledgements—This work was supported by a project grant to Alan Johnston from the Wellcome Trust, Peter McOwan is supported by a Wellcome Fellowship in Mathematical Biology.